FEATURE ARTICLE

Biodegradation of carbon nanohorns in macrophage cells†

Minfang Zhang,*[a] Mei Yang,[a] Cyrill Bussy,[b] Sumio Iijima,[a,c] Kostas Kostarelos[b] and Masako Yudasaka*[a]

With the rapid developments in the medical applications of carbon nanomaterials such as carbon nanohorns (CNHs), carbon nanotubes, and graphene based nanomaterials, understanding the long-term fate, health impact, excretion, and degradation of these materials has become crucial. Herein, the *in vitro* biodegradation of CNHs was determined using a non-cellular enzymatic oxidation method and two types of macrophage cell lines. Approximately 60% of the CNHs was degraded within 24 h in a phosphate buffer solution containing myeloperoxidase. Furthermore, approximately 30% of the CNHs was degraded by both RAW 264.7 and THP-1 macrophage cells within 9 days. Inflammation markers such as pro-inflammatory cytokines interleukin 6 and tumor necrosis factor α were not induced by exposure to CNHs. However, reactive oxygen species were generated by the macrophage cells after uptake of CNHs, suggesting that these species were actively involved in the degradation of the nanomaterials rather than in an inflammatory pathway induction.

1. Introduction

Carbon nanomaterials such as carbon nanohorns (CNHs),[1] carbon nanotubes (CNTs),[2,3] and nanographenes[4,5] possess many interesting properties and potential applications in the development of optics and electronics.[6] Nanocarbons also have potential applications in nanomedicine; for example, CNTs and CNHs can be excellent carriers in drug delivery systems,[7–13] or useful as photo-thermal agents for hyperthermia therapy.[14–18] Although CNTs and CNHs have low toxicity,[19–21] they are still viewed with skepticism because of their accumulation in cells of the mononuclear phagocytic system such as macrophages and their incomplete excretion or clearance from the tissue once administered to animals.[22–25] In addition, the long term fate of accumulated nanomaterials and the impact of their accumulation in tissues have been scarcely investigated. Therefore, evaluating and characterizing

[a]Nanotube Research Center, National Institute of Advanced Industrial Science and Technology (AIST), 1-1-1 Higashi, Tsukuba, Ibaraki 305-8565, Japan.
E-mail: m-zhang@aist.go.jp, m-yudasaka@aist.go.jp; Fax: +81 29861 6920;
Tel: +81 29861 6758
[b]Nanomedicine Lab, Center for Tissue Injury and Repair, Institute of Inflammation and Repair, and National Graphene Institute, The University of Manchester, Manchester M13 9PT, UK. E-mail: cyrill.bussy@manchester.ac.uk,
kostas.kostarelos@manchester.ac.uk; Tel: +44 (0)16127 50215
[c]Meijo University, 1-501 Shiogamaguchi, Tenpaku-ku, Nagoya 468-8502, Japan.
E-mail: iijimas@meijo-u.ac.jp
†Electronic supplementary information (ESI) available. See DOI: 10.1039/c4nr06175f

the potential degradation of carbon nanomaterials in professional phagocytes such as macrophages is crucial to understand both their safety and potential use in nanomedical applications.

Historically, it was generally believed that carbon nanomaterials could not be degraded in tissues due to their stable and inert graphitic structures; however, recent studies have shown that peroxidase enzyme-based processes can lead to the oxidation and biodegradation of CNTs and graphene.[26–31] Oxidized single-wall carbon nanotubes were degraded in stimulated neutrophils without causing obvious pulmonary inflammation when the products of degradation were instilled in the lungs.[28] In addition, it was shown that these same materials can also be directly degraded in the lungs of mice after pharyngeal aspiration.[32] Following stereotactic administration into the brain cortex, amino-functionalized multiwalled carbon nanotubes were also partially degraded in mice,[33] and a long-term study of tangled oxidized multiwalled carbon nanotubes in rat subcutaneous tissue showed that the majority of agglomerates located outside macrophage cells did not undergo degradation, whereas the small agglomerates inside macrophages were degraded gradually.[34] However, only a few *in vitro* studies on CNT biodegradability have been reported to date, and details of the degradation of CNTs in macrophage cells are still scarce. Kagan *et al.* have first demonstrated that monocyte-derived macrophages freshly isolated from healthy adults can degrade oxidized CNTs,[28] and have recently reported in a follow-up study that the oxidative degradation of oxidized CNTs in PMA activated THP-1 macrophages

actually took place mainly *via* a 'super-oxide/NO* → peroxy-nitrite'-driven oxidative pathway.[35]

To our knowledge, the biodegradation of CNHs, which has high potential in the field of nanomedicine, has not yet been investigated. In our previous mouse study, approximately 40% of a dose of intravenously injected CNHs was cleared from the body after 1 month, of which 15% was excreted in feces and the remaining 25% was thought to first accumulate and then degrade in macrophages of the liver,[24] although this proposal has not yet been confirmed. To test the hypothesis of macrophage-mediated degradation of CNHs, we investigated here the biodegradability of CNHs in a non-cellular model as well as in two cell lines, namely RAW 264.7 mouse leukemia macrophage cells and THP-1 human leukemia cells. The results confirmed that CNHs are degraded by both myeloperoxidase (MPO)-catalyzed oxidation and by macrophage cells, as previously reported for CNTs.[28,30] An estimated 30% of the CNHs were degraded in the RAW 264.7 and THP-1 macrophages. To determine their roles in the degradation of CNHs, the induction of reactive oxygen species (ROS) and cytokines in macrophages by CNHs was also investigated. The results presented here contribute to the current understanding of the biodegradation of other carbon nanomaterials, particularly those that are free from impurities, such as metals.[1,36]

2. Results

2.1. Degradation of CNHs by enzymatic oxidation

Previous studies have shown that only oxidized CNTs are degraded;[28,29] therefore, oxidized CNHs generated by light-assisted oxidation with H_2O_2 were used throughout the study, unless otherwise specified.[37] A thermogravimetric analysis of the oxidized CNHs (Fig. S1†) showed that the weight loss between room temperature and 1000 °C in helium was approximately 12%, indicating the creation of abundant oxygenated functional groups, such as carbonyls and carboxylic groups on the surface.[37] The CNHs were then treated with a solution of human MPO supplemented with a low concentration of H_2O_2 (800 μM), which is a little higher than that used in a previous study on MPO-mediated CNT degradability (200 μM).[28] The dark dispersion of the treated CNHs lightened gradually over 24 h, while the dark color of the CNH-dispersion treated with H_2O_2 alone did not change during the same time period (Fig. 1a). Optical absorption measurements[38] showed that the quantity of CNHs decreased by approximately 40 wt% and 60 wt% after treatment with a combination of MPO and H_2O_2 for 5 h and 24 h, respectively (Fig. 1b). Transmission electron microscopy (TEM) images of untreated CNHs (starting materials) showed that they formed aggregates of approximately 100 nm in size and had clearly visible horn-shaped tips (Fig. 2a). In contrast, after enzymatic oxidation for approximately 24 h, the CNHs were severely damaged and the horn-shaped tips and spherical forms had collapsed (Fig. 2b–d). A large amount of non-CNH materials, probably MPO, were also observed in the samples (Fig. 2c).
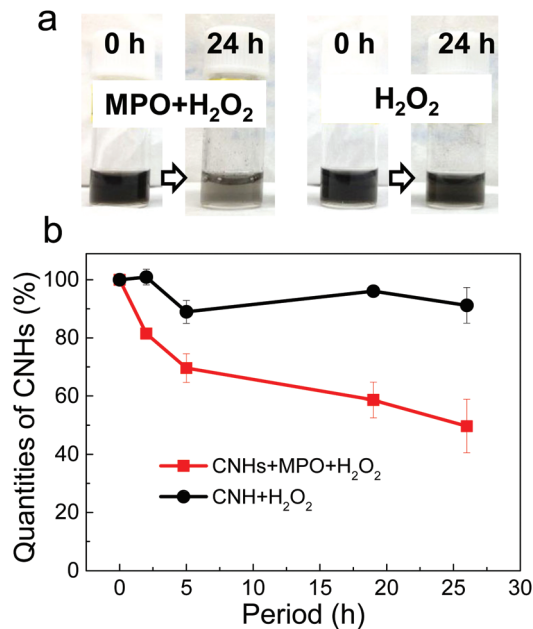

Fig. 1 Human MPO-mediated degradation of CNHs. (a) Photographs of the CNH dispersions before and after treatment with a low concentration of H_2O_2 and with or without MPO. (b) The quantities of CNHs after treatment with H_2O_2 and with or without MPO for the indicated times. The quantities of CNHs were estimated based on the optical absorbance at 700 nm. Data represent the percentage of CNHs relative to the starting concentration and are expressed as the mean ± SD of n = 3 independent replicates.

The structures of imperfectly-degraded CNHs (Fig. 2c and d) were similar in appearance to amorphous carbon or graphite-like carbon nanoparticles.[39]

2.2. Degradation of CNHs in macrophage cells

Next, the cellular degradation of CNHs in mouse leukemia RAW 264.7 macrophage cells was investigated. The cells were incubated with CNHs (10 μg ml^{-1}) for 24 h, washed with phosphate-buffered saline (PBS), and then re-seeded with CNH-free fresh medium for a further period of 9 days (recovery period). Confocal microscopy differential interference contrast (DIC) images revealed that a lot of the CNHs, which appeared as black spots inside the cells, were taken up by the macrophages after the 24 h incubation (Fig. 3a). Most of the CNHs were located in lysosomes, as confirmed by staining the cells with LysoTracker Red DND-99 dye (Fig. S2†), as well as by the results of our previous study.[40] The black spots representing the CNHs disappeared gradually during the recovery period (from days 1 to 9) and optical absorption measurements revealed that approximately 30% of the CNHs inside the cells disappeared within this time period (Fig. 3b).

The same process was then performed using macrophages derived from human leukemia THP-1 cells. Prior to the addition of CNHs, the cells were differentiated from monocytes to macrophages by adding phorbol 12-myristate 13-acetate (PMA) to the culture medium.[41] After differentiation, the number of cells was stable due to a loss of their ability to
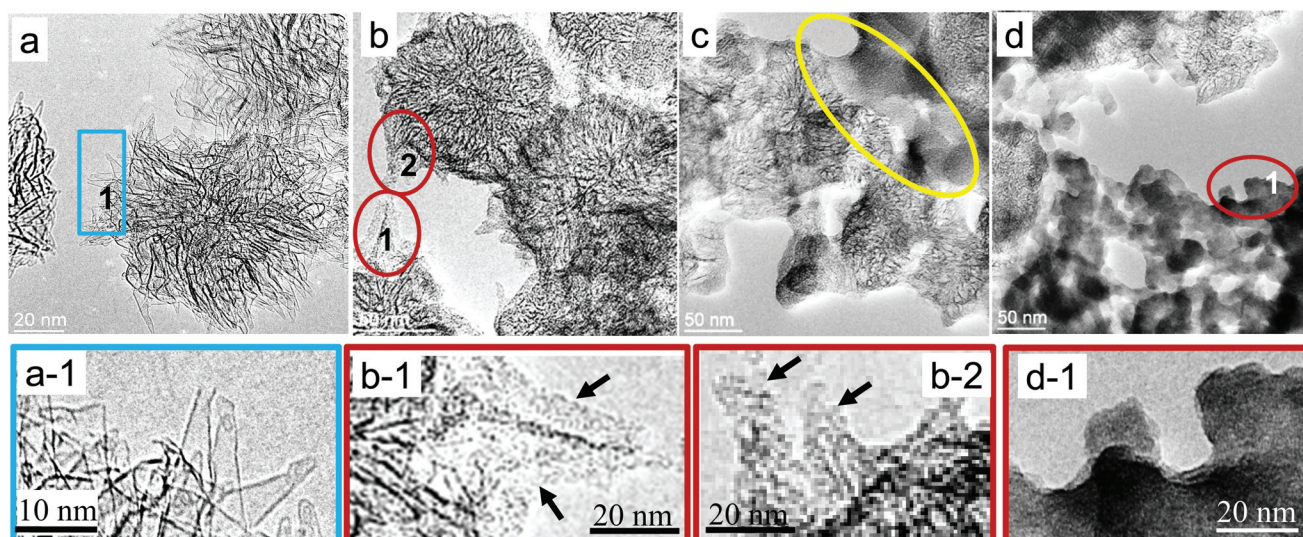
Fig. 2 (a–d) TEM images of CNHs before (a) and after (b–d) enzymatic oxidation for 24 h. The inset panels (a-1, b-1, b-2, and d-1) show magnified images. The arrows indicate the structural changes in the CNHs after treatment with MPO and H_2O_2. (c) Some amorphous-like materials were probably MPO-molecules' aggregates (yellow ellipse).
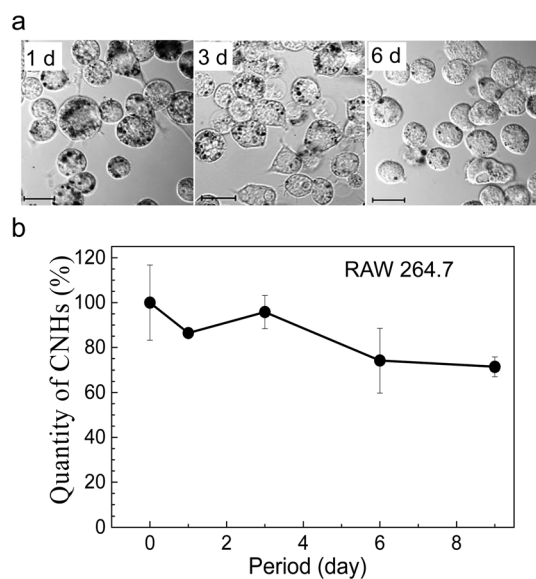

Fig. 3 Degradation of CNHs in RAW 264.7 macrophages. The cells were incubated with CNHs for 24 h and then re-seeded in a fresh medium and incubated for a further period of 1–9 days. (a) Confocal microscopy DIC images of RAW 264.7 cells at days 1, 3, and 6. The black spots represent CNHs. Scale bar, 20 μm. (b) The quantities of CNHs inside the cells on days 0–9, which were estimated based on the optical absorbance at 700 nm. Data represent the percentage of CNHs relative to the starting concentration and are expressed as the mean ± SD of n = 3 independent replicates.

Fig. 4 Degradation of CNHs in macrophages derived from THP-1 cells. The cells were differentiated by adding PMA, incubated with CNHs for 24 h, and then re-seeded in a fresh medium and incubated for a further period of 1–9 days. (a) Confocal microscopy DIC images of THP-1 cells at days 1, 3, and 6. The black spots represent CNHs. (b) The quantities of CNHs inside the cells on days 1–9. Data represent the percentage of CNHs relative to the starting concentration and are expressed as the mean ± SD of n = 3 independent replicates.

replicate (Fig. S3†), which was helpful in evaluating the degradation of the CNHs. Confocal microscopy DIC analyses showed that, similar to the observations in RAW 264.7 cells, the number and size of the black particles (representing CNHs) decreased gradually over time after the THP-1 cells were
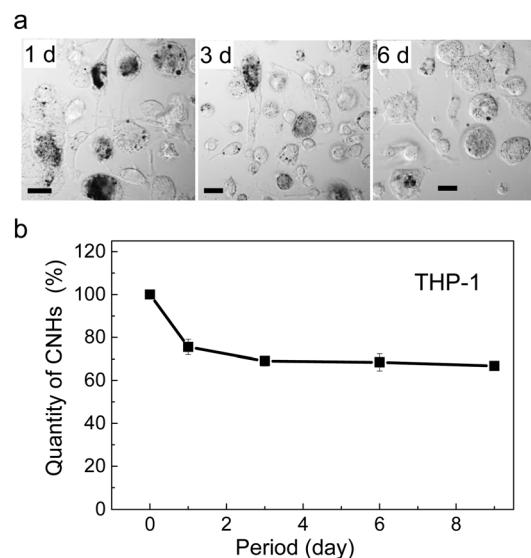
incubated with CNHs for 24 h and then re-seeded with fresh CNH-free medium and observed for a further period of 9 days (Fig. 4a). Optical absorption measurements revealed that approximately 30% of the CNHs inside the THP-1 cells disappeared within the 9-day observation period, which was consistent with the results obtained for RAW 264.7 cells.
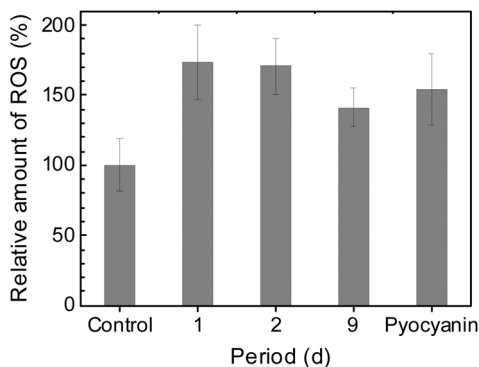
Fig. 5 Generation of ROS in RAW 264.7 macrophages induced by incubation with CNHs. The cells were incubated with CNHs for 24 h and then observed for 9 days. Naïve cells were not treated with CNHs and treatment of the cells with pyocyanin (200 μM) was used as a positive control. Data represent the percentage of ROS relative to that in the untreated naïve cells and are expressed as the mean ± SD of n = 3 independent replicates.

2.3. ROS generation

We have previously reported that after the uptake of CNHs by RAW 264.7 macrophages, ROS were generated.[40] Despite their role in the oxidative stress response to nanomaterial exposure, ROS are known to be important oxidizing agents for enzymatic oxidation degradation;[28,42] therefore, the ROS levels in naïve and CNH-treated RAW 264.7 cells were compared. The ROS level in the cells incubated with CNHs (10 μg ml^{-1}) for 24 h was approximately 1.5-fold higher than that in untreated naïve cells and was stable over the 9 days observation period (Fig. 5). The amounts of ROS released from THP-1 cells incubated with CNHs for 24 h or 72 h were also higher than those released by the corresponding untreated naïve cells (Fig. S4†).

2.4. Cytokine detection

Next, the amounts of the interleukin 6 (IL-6) and tumor necrosis factor α (TNF-α) cytokines released from RAW 264.7 macrophage cells incubated with CNHs (0, 10, or 100 μg ml^{-1}) were measured. For both cytokines, there were no obvious differences between the amounts released by the untreated and CNH-treated cells (Fig. 6).
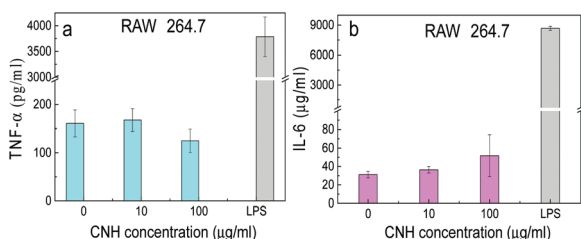

Fig. 6 (a, b) Generation of TNF-α (a) and IL-6 (b) by RAW 264.7 macrophages induced by incubation with the indicated concentration of CNHs for 24 h. Lipopolysaccharide (LPS, 20 μg ml^{-1}) was used as a positive control. Data are expressed as the mean ± SD of n = 6 independent replicates.

3. Discussion

3.1. CNHs are less susceptible to enzymatic oxidation-induced degradation than CNTs

Although some of the CNHs were degraded by MPO-catalyzed oxidation in the non-cellular experiment, the degradation was incomplete; in contrast, in a previous study, CNTs were completely degraded within 24 h following a similar MPO-H$_2$O$_2$ process.[28] In addition, although the concentrations of MPO (50 μg ml^{-1}) and H$_2$O$_2$ (800 μM) used here were higher than those used in the CNT study (MPO, 30 μg ml^{-1}; H$_2$O$_2$, 200 μM), 40% of the CNHs remained intact after 24 h. MPO generates hypochlorous acid from H$_2$O$_2$ and chlorine ions,[41] therefore the quantity of chlorine ions is an important factor for MPO-catalyzed CNT degradation.[28,41] Here, we used PBS containing 137 mM NaCl, which is higher than that used in the previous study of CNT degradation (approximately 200 μM NaCl),[28] suggesting that the concentration of NaCl employed here should have been sufficient to promote MPO-catalyzed CNH degradation in a fashion similar to the MPO mediated CNT degradation.

Because oxidized CNTs are more susceptible to degradation than non-oxidized CNTs,[28,29] we also investigated the MPO-catalyzed degradation of CNHs that were strongly oxidized via pre-treatment with H$_2$SO$_4$ and HNO$_3$ (S-CNH) instead of being pre-oxidized with H$_2$O$_2$ as for the CNHs described herein.[38] The strongly oxidized CNHs presented more defects and more oxygenated groups than those pre-treated with H$_2$O$_2$ (Fig. S1, S5 and S6†); however, MPO-catalyzed degradation of the S-CNHs was not enhanced by the strong acid pre-treatment (Fig. S7†). Taken together, these results suggest that the lower susceptibility of CNHs to enzymatic oxidation-induced degradation compared to CNTs may be due to a weaker effect of the MPO catalytic sites and/or the specific structural characteristics of CNHs.

The tyrosine residues at positions 293 and 313 of MPO, which are located at the proximal end of the heme group, are the catalytic sites of the enzyme.[43] Simulations have, moreover, revealed that the potential sites of interaction of MPO with oxidized CNTs are also located at the proximal end of the MPO heme group where the carboxyl groups of CNTs interact with positively charged tyrosines 293 and 313.[28] However, considering the molecular modeling analyses performed for CNTs,[28] we believe that the morphology and size of CNHs would preclude their location near the catalytic site of MPO. Indeed, this interaction would likely be sterically restricted because CNHs form dense spherical aggregates that exhibit large overall curvatures with diameters of approximately 100 nm. To test this hypothesis, CNHs were mixed with 50 μg of MPO for 1–5 h, leading to a concentration of MPO attached to the CNHs of about 50–60 μg mg^{-1} (Fig. S8†), which is lower than that described previously for CNTs (180 μg mg^{-1}),[28] suggesting that the interaction of MPO with CNHs is weaker than that with CNTs. In addition, as mentioned above, enrichment of the carboxyl groups via a strong acid pre-treatment did not enhance the degradation of the acid-treated CNHs by MPO (Fig. S7†),

suggesting that the interaction between CNH and MPO, in contrast to CNTs, is not likely bound to the presence of carboxyl groups.

The non-degraded CNHs lost their tubular structures (Fig. 2) and were similar in appearance to that of CNHs after a 70% weight loss caused by combustion in oxygen from room temperature to 590 °C,[39] indicating that the biodegradation may occur from the periphery to the center of the aggregates. Nanohorn tubules are horn-shaped structures with diameters of approximately 2–5 nm that have structural defects (pentagonal and heptagonal rings).[1] The parts of CNHs with thinner diameters and defect sites are easily combusted and approximately 40% of CNHs containing graphite-like thin sheets in the centers of aggregates are difficult to combust at temperatures lower than 590 °C.[39] We propose that the easily combusted sites were enzymatically degraded early, whereas the parts that were difficult to combust accounted for the remaining (non-degraded) CNH material. This also was the reason why that the degradation rates of CNHs by MPO and H_2O_2 became very low after treatment for about 5 hours.

The presence of metal impurities in carbon nanomaterials might be another reason for the lower susceptibility of CNHs to degradation. CNHs do not contain any metals, whereas CNTs contain metal catalyst particles that cannot be completely removed. In fact, consistent with the results of a previous CNT study,[27] the addition of $FeCl_3$ catalyzed the degradation of CNHs (Fig. S8†), suggesting that the presence of metallic ions may enhance the non-cellular and cellular degradation of carbon nanomaterials *via* a Fenton reaction.

3.2. Causal relationship between ROS and CNH degradation

ROS are a family of strong oxidizing agents that can promote CNT degradation.[28,42] Here, ROS were generated by RAW 264.7 cells in response to CNH exposure, and the elevated ROS levels were stable for the entire 9-day observation period (Fig. 5), which presumably sustained a continuous degradation of the CNHs for the same period as evidenced in Fig. 3. The slight decrease in ROS levels over time could be first explained by their consumption by the enzymatic oxidation-induced degradation process. However, as degradation of CNHs progressed, fewer CNHs remained to induce further production of ROS, leading to a decrease of those species over time, as observed in Fig. 5, and ultimately to a reduction of the degradation process rate as in Fig. 4. In addition, the ROS levels in the two types of macrophage cells used here were not high enough to induce the release of proinflammatory cytokines (Fig. 6).

4.   Conclusion

This study investigated the biodegradation of CNHs by MPO catalyzed oxidation in both a non-cellular model and *in vitro* using mouse and human monocyte-derived macrophages. Approximately 60% and 30% of the CNHs were degraded by MPO catalyzed oxidation and macrophage cells, respectively. Incubation of macrophage cells with CNHs induced ROS

release that led to degradation of the nanomaterials but not to an inflammatory response.

5.   Experimental section

5.1.   Degradation of CNHs by enzymatic oxidation

As grown CNHs that were produced by CO_2 laser ablation of graphite without the use of metal catalysts[1,36] underwent light-assisted oxidation with H_2O_2 to enhance their hydrophilic properties.[37] The process used for MPO oxidation-based degradation of CNHs was similar to that described previously for CNTs.[28] After light-assisted oxidation with H_2O_2, the CNHs were dispersed in water at a concentration of approximately 1 mg ml^{-1}; this dispersion (0.3 ml) was mixed with Dulbecco's PBS (0.7 ml) (Sigma) containing MPO (50 μg) from human neutrophils (Fisher Scientific) and H_2O_2 (10 μl of 80 mM). The final concentration of H_2O_2 in the CNH suspension was approximately 800 μM. The reaction mixture was maintained at 37 °C for 3 days. To replenish their levels, additional MPO (50 μg) was added after 5 h and additional H_2O_2 (10 μl of 80 mM) was added after 5 h, 24 h, and 30 h. The amount of CNHs in the reaction mixture was estimated based on light absorbance at 700 nm using a Lambda 1050 UV-Vis-NIR spectrophotometer (PerkinElmer Japan Co., Ltd).[38] The structures were observed using a TEM (Topcon 002B).

5.2.   Degradation of CNHs by murine RAW 264.7 macrophages

Mouse leukemic monocyte macrophage RAW 264.7 cells (European Collection of Cell Cultures) were cultured in RPMI-1640 medium (Invitrogen) containing 10% fetal bovine serum (Gibco) and streptomycin/penicillin (Gibco) at 37 °C under a 5% CO_2 atmosphere. The cells (3×10^5) were seeded in 10 ml dishes (Iwaki) and incubated for 24 h. The culture medium was then replaced with fresh medium containing CNHs (0.01 mg ml^{-1}) and the cells were incubated for a further 24 h, after which the medium was removed and a PBS rinse was performed to eliminate CNHs not taken up by the cells. The cells were then detached from the culture dishes by adding 0.25% Trypsin-EDTA, re-suspended in culture medium, seeded into 6-well plates (3 ml per well, 5×10^5 cells ml^{-1}), and cultured for 1–9 days. The amounts of CNHs inside the cells were estimated by optical absorption measurements.[38] Briefly, we removed the culture medium, and then added CelLytic M solution (1 ml) (Sigma, C2978) to each well. After incubation of the cells for at least 1 h, the cell dispersions were collected and ultra-sonicated (Vibra cell, Sonics Inc.) at a power of approximately 300 W for 10 min. The optical absorbance of cell lysis and the culture media was then measured using a Lambda 1050 UV-Vis-NIR spectrophotometer. The quantities of CNHs were estimated based on the optical absorption intensities at 700 nm using a calibration curve.[38]

5.3. Degradation of CNHs by human leukemia THP-1 macrophages

Human monocytic THP-1 cells (ATCC) were cultured in RPMI-1640 medium supplemented with 10% fetal bovine serum, 1% L-glutamine and streptomycin/penicillin (Gibco) at 37 °C under a 5% CO_2 atmosphere. To induce differentiation, the cells (2×10^6 cells ml^{-1}) were seeded in culture medium containing PMA (50 ng ml^{-1}) (Wako),[41] which is hereafter referred to as complete medium. After incubation for 24 h, the non-adherent cells were removed by aspiration and the adherent cells were incubated in fresh complete culture medium containing CNHs (10 μg ml^{-1}). After a further incubation for 24 h, the cells were washed with PBS and detached from the culture dishes by adding 0.25% Trypsin-EDTA. After centrifugation, the cells were re-suspended in complete medium and seeded into 6-well plates (3 ml per well, 6×10^5 cells ml^{-1}). The amounts of CNHs in the cells were estimated as described for the RAW 264.7 cells.

5.4. ROS detection

The ROS detection was performed as described previously,[44] with some minor modifications by M. Yang et al. (unpublished data). Briefly, CNH-treated RAW 264.7 or THP-1 cells were rinsed with PBS and incubated with 2′,7′-dichlorodihydrofluorescein diacetate (2 ml of 10 μM) (Life Technologies) at 37 °C for 30 min. The cells were then washed three times with PBS and lysed with CelLytic M reagent containing a protease inhibitor cocktail. After centrifugation of the cell lysate at 18 000g for 10 min, the supernatants were collected and examined using a fluorescence spectrophotometer (Fluorolog 3, Horiba, Ltd) at excitation and emission wavelengths of 488 nm and 525 nm, respectively. The fluorescence intensity was normalized to the amount of protein and divided by that in the naïve cells, and then the values for three wells were averaged. The amount of protein in the cell lysate was measured using Bradford reagent (Sigma-Aldrich, B6916), according to the manufacturer's instructions. As a positive control, the cells were incubated with medium (2 ml) containing pyocyanin (200 μM) for approximately 3 h.

5.5. Cytokine measurement

The cell lysates obtained from CNH-treated RAW 264.7 cells were used for cytokine measurements. The IL-6 and TNF-α levels were measured using ELISA kits (Thermo Inc.) according to the manufacturer's instructions. As a positive control, the cells were incubated with medium (2 ml) containing lipopolysaccharide (LPS, 20 μg ml^{-1}) for approximately 24 h.

References

1 S. Iijima, M. Yudasaka, R. Yamada, S. Bandow, K. Suenaga, F. Kokai and K. Takahashi, *Chem. Phys. Lett.*, 1999, **309**, 165.
2 S. Iijima, *Nature*, 1991, **354**, 56.
3 S. Iijima and T. Ichihashi, *Nature*, 1993, **363**, 603.
4 D. V. Kosynkin, A. L. Higginbotham, A. Sinitskii, J. R. Lomeda, A. Dimiev, B. K. Price and J. M. Tour, *Nature*, 2009, **458**, 872.
5 L. Jiao, L. Zhang, X. Wang, G. Diankov and H. Dai, *Nature*, 2009, **458**, 877.
6 A. Jorio, G. Dresselhaus and M. S. Dressehaus, *Carbon Nanotubes*, Springer, New York, USA, 2008.
7 P. Feazell, N. Nakayama, H. Dai and S. J. Lippard, *J. Am. Chem. Soc.*, 2007, **129**, 8438.
8 Z. Liu, X. Sun, N. Nakayama and H. Dai, *ACS Nano*, 2007, **1**, 50.
9 A. Bianco, K. Kostarelos and M. Prato, *Curr. Opin. Chem. Biol.*, 2005, **9**, 674.
10 Z. Liu, K. Chen, C. Davis, S. Sherlock, Q. Cao, X. Chen and H. Dai, *Cancer Res.*, 2008, **68**, 6652.
11 T. Murakami, K. Ajima, J. Miyawaki, M. Yudasaka, S. Iijima and K. Shiba, *Mol. Pharm.*, 2004, **1**, 399.
12 K. Ajima, T. Murakami, Y. Mizoguchi, K. Tsuchida, T. Ichihashi, S. Iijima and M. Yudasaka, *ACS Nano*, 2008, **10**, 2057.
13 K. Yang, L. Feng, X. Shi and Z. Liu, *Chem. Soc. Rev.*, 2013, **42**, 530.
14 N. W. S. Kam, M. O'Connel, J. Wisdom and H. Dai, *Proc. Natl. Acad. Sci. U. S. A.*, 2005, **102**, 11600.
15 M. Zhang, T. Murakami, K. Ajima, K. Tsuchida, A. Sandanayaka, O. Ito, S. Iijima and M. Yudasaka, *Proc. Natl. Acad. Sci. U. S. A.*, 2008, **105**, 14773.
16 H. Moon, S. Lee and H. Choi, *ACS Nano*, 2009, **3**, 3707.
17 J. Robinson, K. Welsher, S. Tabakman, S. Sherlock, H. Wang, R. Luong and H. Dai, *Nano Res.*, 2010, **3**, 779.
18 K. Yang, S. Zhang, G. Zhang, X. Sun, S. Lee and Z. Liu, *Nano Lett.*, 2010, **10**, 3318.
19 L. Yan, F. Zhao, S. Li, Z. Hu and Y. Zhao, *Nanoscale*, 2010, **3**, 362.
20 S. Jain, V. Thakara, M. Das, C. Godugu, A. Jain, R. Mathur, K. Chuttani and A. Mishra, *Chem. Res. Toxicol.*, 2011, **24**, 2028.
21 J. Miyawaki, T. Azami, Y. Kubo and S. Iijima, *ACS Nano*, 2008, **2**, 213.
22 Z. Liu, D. Corrine, W. Cai, L. He, X. Chen and H. Dai, *Proc. Natl. Acad. Sci. U. S. A.*, 2008, **105**, 1410.
23 J. Miyawaki, S. Matsumura, R. Yuge, T. Murakami, S. Sato, A. Tomida, T. Tsuruo, T. Ichihashi, T. Fujinami, H. Irie,

K. Tsuchida, S. Iijima, K. Shiba and M. Yudasaka, *ACS Nano*, 2009, **3**, 1399.

24 M. Zhang, Y. Tahara, M. Yang, X. Zhou, S. Iijima and M. Yudasaka, *Adv. Healthcare Mater.*, 2014, **3**, 239.

25 K. Al-Jamal, A. Nunes, L. Methven, H. Ali-Boucetta, S. Li, F. Toma, M. A. Herrero, W. Al-Jamal, H. M. Eikelder, J. Foster, S. Mather, M. Prato, A. Bianco and K. Kostarelos, *Angew. Chem., Int. Ed.*, 2012, **51**, 6389.

26 B. L. Allen, P. D. Kichambare, P. Gou, I. I. Vlasova, A. A. Kapralov, N. Konduru, V. E. Kagan and A. Star, *Nano Lett.*, 2008, **8**, 3899.

27 B. L. Allen, G. P. Kotchey, Y. Chen, N. V. K. Yanamala, J. Klein-Seetharaman, V. E. Kagan and A. Star, *J. Am. Chem. Soc.*, 2009, **131**, 17194.

28 V. Kagan, N. Konduru, W. Feng, B. Allen, J. Conroy, Y. Volkov, I. Vlasova, N. Belikova, N. Yanamala, A. Kapralov, Y. Tyurina, J. Shi, E. Kisin, A. Murray, J. Franks, D. Stolz, P. Gou, J. Klein-Seetharaman, B. Fadeel, A. Star and A. Shvedova, *Nat. Nanotechnol.*, 2010, **5**, 354.

29 Y. Zhao, B. Allen and A. Star, *J. Phys. Chem. A*, 2011, **115**, 9536.

30 G. P. Kotchey, Y. Zhao, V. E. Kagan and A. Star, *Adv. Drug Delivery Rev.*, 2013, **65**, 1921.

31 G. P. Kotchey, S. A. Hasan, A. A. Kapralov, S. H. Ha, K. Kim, A. A. Shvedova, V. E. Kagan and A. Star, *Acc. Chem. Res.*, 2012, **45**, 1770.

32 A. Shvedova, A. Kapralov, W. Feng, E. Kisin, A. Murray, R. Mercer, C. St. Croix, M. Lang, S. Watkins, N. Konduru, B. Allen, J. Conroy, G. Kotchey, B. Mohamed, A. Meade, Y. Volkov, A. Star, B. Fadeel and V. Kagan, *PLoS One*, 2012, **7**, e30923.

33 A. Nunes, C. Bussy, L. Gherardini, M. Meneghetti, M. A. Herrero, A. Bianco, M. Prato, T. Pizzorusso, K. Al-Jamal and K. Kostarelos, *Nanomedicine*, 2012, **7**, 1485.

34 Y. Sato, A. Yokoyama, Y. Nodasaka, T. Kohgo, K. Motomiya, H. Matsumoto, E. Nakazawa, T. Numata, M. Zhang, M. Yudasaka, H. Hara, R. Araki, O. Tsukamoto, H. Saito, T. Kamino, F. Watari and K. Tohji, *Sci. Rep.*, 2013, **3**, 2516, DOI: 10.1038/srep0216.

35 V. E. Kagan, A. A. Kapralov, C. M. St. Croix, S. C. Watkins, E. R. Kisin, G. P. Kotchey, K. Balasubramanian, I. I. Vlasova, J. Yu, K. Kim, W. Seo, R. K. Mallampalli, A. Star and A. A. Shvedova, *ACS Nano*, 2014, **8**, 5610.

36 T. Azami, D. Kasuya, R. Yuge, M. Yudasaka, S. Iijima, T. Yoshitake and Y. Kubo, *J. Phys. Chem. C*, 2008, **112**, 1330.

37 M. Zhang, M. Yudasaka, K. Ajima, J. Miyawaki and S. Iijima, *ACS Nano*, 2007, **1**, 265.

38 M. Zhang, X. Zhou, S. Iijima and M. Yudasaka, *Small*, 2012, **8**, 2524.

39 M. Irie, M. Nakamura, M. Zhang, R. Yuge, S. Iijima and M. Yudasaka, *Chem. Phys. Lett.*, 2010, **500**, 96.

40 Y. Tahara, M. Nakamura, M. Yang, M. Zhang, S. Iijima and M. Yudasaka, *Biomaterials*, 2012, **33**, 2762.

41 E. Park, H. Jung, H. Yang, M. Yoo, C. Kim and K. Kim, *Inflammation Res.*, 2007, **56**, 45.

42 I. I. Vlasova, A. V. Sokolov, A. V. Chekanov, V. A. Kostevich and V. B. Vasilyev, *Russ. J. Bioorg. Chem.*, 2011, **37**, 453.

43 M. L. Olivier and R. O. Paul, *Biochem. Biophys. Res. Commun.*, 2000, **1**, 199.

44 R. Foldbjerg, P. Olesen, M. Hougaard, D. Dang, H. Hoffmann and H. Autrup, *Toxicol. Lett.*, 2009, **190**, 156.